International Journal of Innovative Computing, Information and Control
Volume **18**, Number **2**, April **2022**

ICIC International ©2022 ISSN 1349-4198
pp. **591–605**

WAVELENGTH PATH MANAGEMENT APPLICATIONS FOR RECONFIGURABLE ARRAYED WAVEGUIDE GRATING – STAR NETWORK

Kento Oyama[1], Minoru Yamaguchi[1], Osanori Koyama[1,*], Keigo Mino[1]
Akihiro Imae[1], Ippei Tomo[2], Kanami Ikeda[1] and Makoto Yamada[1]

[1]Graduate School of Engineering
[2]College of Engineering
Osaka Prefecture University
Gakuen-cho 1-1, Naka-ku, Sakai, Osaka 599-8531, Japan
{ md104012; szb01158; sab01019 }@edu.osakafu-u.ac.jp; m.yamaguchi@m.ieice.org
{ nf101345; kanami; myamada }@eis.osakafu-u.ac.jp
*Corresponding author: koyama@eis.osakafu-u.ac.jp

Received September 2021; revised January 2022

Abstract. *We have proposed an arrayed waveguide grating router (AWGR) network with a loopback function by optical switches (OSWs) that are located on optical nodes that allow the arbitrarily reconfigured wavelength path architecture. In order to easily manage the architecture, we have also proposed the method expressed network topology so that it could also calculate network information based on topologies and be helpful for a network controller that needed topology information. However, since the proposed method outputs the wavelength path from the OSW state, it is impossible to calculate the required OSW states from the information between the nodes where the wavelength path is multiplexed. If we employ the inverse matrix calculation to know the required OSW states, we must know all matrices except OSW state in advance, which is unrealistic. Thus, in this study, our proposed method simulates the case that the target network has only the required path and, calculates wavelength path routes and required OSW states. In addition, from the network management perspective, we need an interface easy for network administrators to manage, but previous proposals have only considered basic calculation methods. In this study, we develop an application with a graphical user interface for network administrators, which can show the required wavelength path and OSW states when the information between the nodes where the wavelength paths are multiplexed is inputted into the application.*
Keywords: Path planning, Wavelength routing, Network topology

1. **Introduction.** Recently, communication traffic in data centers has been increasing due to the rapid increase in the use of cloud applications. The data center traffic was expected to increase from 6.0 ZB per year in 2016 to 19.5 ZB per year in 2021 [1]. Thus, data center networks are required to have low-power consumption, low latency, capacity scalability, and flexibility. For communication capacity expansion, various multiplexing technologies, e.g., wavelength division multiplexing (WDM) and space division multiplexing, have been introduced in information communication networks [2,3]. WDMs, such as arrayed waveguide grating (AWG), have also been employed in data center networks to realize low-power and low-latency communication networks. An AWG-STAR network, which uses AWGs as wavelength routers and can logically realize a full-mesh wavelength path configuration with a physical star topology, has been studied [4-6]. Previously, we

DOI: 10.24507/ijicic.18.02.591

proposed a network architecture that can reconfigure wavelength paths using an AWG router (AWGR) for relatively small-scale networks, which was possible because the wavelength path topology of the AWG-STAR network is generally fixed, despite fluctuations in traffic demands [7].

Figure 1 shows a scheme of the proposed network. The figure shows how the nodes and AWGR are connected. The nodes comprise a multiplexer (MUX), a demultiplexer (DEMUX), optical switches (OSWs) corresponding to each wavelength, and a layer-3 switch (L3SW) that can transmit WDM signals. MUX/DEMUX is needed to connect the WDM network and L3SW with colored interfaces. OSWs are essential components that enable reconfiguring the topology by switching an optical path from connection with AWGR and L3SW to connection with the output and input ports of AWGR. Flexible optical path relocation by OSW before L3SW's routing enables low latency and efficient capacity usage. Signals transmitted from nodes are input into the AWGR. These signals are routed to each output port following the AWGR wavelength routing characteristics. The signals routed by the AWGR are received at each node when the OSW state is C_{PT} and input again to the AWGR by looping back the signal when the OSW state is C_{LB} (Figure 1). Consequently, the optical path is relocated by routing the signal again. Figure 1 shows an example where a 4×4 AWGR and 3 wavelengths are used. In this case, λ_1 in Node 2 and λ_3 in Node 4 are looped back, and the others are the path through, resulting in a threefold increase in the number of wavelength paths from Nodes 3 to 1. Further, we demonstrated that the multiple wavelength paths could be dynamically relocated in the proposed AWG-STAR network [8-11].

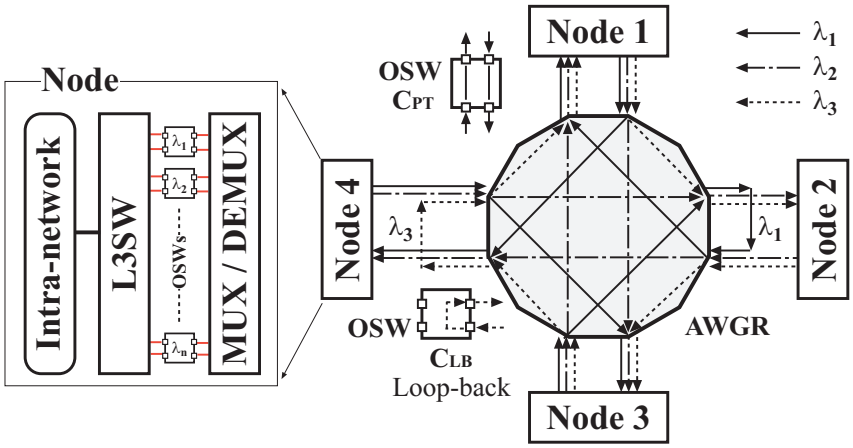

FIGURE 1. Scheme of AWG-STAR network with loopback function

2. **Conventional Matrix Calculation.** The wavelength path relocation in the proposed AWG-STAR network complicates the wavelength path topology, thereby making it extremely difficult to manage wavelength path and network capacity. A calculation method for wavelength path topology using a wavelength transfer matrix was proposed for an AWG-STAR network with fixed wavelength path topology [12,13]. However, the calculation method could not be directly applied to the proposed AWG-STAR network because it could not express the relocation of a specific wavelength path. Therefore, we proposed a calculation method that could calculate path topology, which includes the transit nodes and optical margins in the AWG-STAR network, with a loopback function [14]. We briefly describe how to calculate the wavelength path of the proposed AWG-STAR network using matrix calculation. The matrix $\boldsymbol{O}$, which represents the connection between each node by wavelength path, can be calculated using matrices $\boldsymbol{I}$, $\boldsymbol{L}$, and $\boldsymbol{S}$.

Each matrix is an $N \times N$ matrix, where N is the number of nodes in the network. The number of wavelengths used in the network is also N. Here, $\boldsymbol{I}$, $\boldsymbol{O}$, and $\boldsymbol{S}$ represent the characteristics of the input wavelength from the nodes to the AWGR, the relationship between the connection nodes and wavelength paths, and the state of an OSW, respectively. Each element $i_{p,q}$, $o_{j,k}$, and $s_{p,q}$ is, respectively, expressed as follows:

$$\begin{aligned} \boldsymbol{I} = (i_{p,q}) \quad & p = 1, \ldots, N\text{: node number} \\ & q = 1, \ldots, N\text{: wavelength number} \end{aligned} \tag{1}$$

$$\begin{aligned} \boldsymbol{O} = (o_{j,k}) \quad & j = 1, \ldots, N\text{: source node number} \\ & k = 1, \ldots, N\text{: destination node number} \end{aligned} \tag{2}$$

$$\begin{aligned} \boldsymbol{S} = (s_{p,q}) \quad & p = 1, \ldots, N\text{: node number} \\ & q = 1, \ldots, N\text{: wavelength number} \end{aligned} \tag{3}$$

where $i_{p,q}$ is the wavelength path of λ_q inputted from Node p to AWGR, $o_{j,k}$ is the number of wavelength paths transmitted from Nodes j to k, and $s_{p,q}$ is the state of an OSW installed in Node p to control λ_q. When the state of the OSW was $\mathrm{C_{PT}}$, $s_{p,q}$ was 0; when the state of OSW was $\mathrm{C_{LB}}$, $s_{p,q}$ was 1. Here, $\boldsymbol{L}$ represents the wavelength transfer matrix. The $\boldsymbol{L}$ rows were source nodes, and the $\boldsymbol{L}$ columns were destination nodes. The entry Λ_r of $\boldsymbol{L}$ indicated a wavelength routed by the routing function of the AWGR. In this study, the AWGR exhibited a cyclic characteristic. Therefore, $\boldsymbol{L}$ and its entries can be expressed as follows:

$$\boldsymbol{L} = \begin{pmatrix} \Lambda_1 & \Lambda_2 & \Lambda_3 & \cdots & \Lambda_r & \cdots & \Lambda_N \\ \Lambda_N & \Lambda_1 & \Lambda_2 & \cdots & \Lambda_{r-1} & \cdots & \Lambda_{N-1} \\ \Lambda_{N-1} & \Lambda_N & \Lambda_1 & \cdots & \Lambda_{r-2} & \cdots & \Lambda_{N-2} \\ \vdots & \vdots & \vdots & \vdots & \vdots & \ddots & \vdots \\ \Lambda_2 & \Lambda_3 & \Lambda_4 & \cdots & \Lambda_{r+1} & \cdots & \Lambda_1 \end{pmatrix} \quad r = 1, 2, \ldots, N \tag{4}$$

where r is the entry number of $\boldsymbol{L}$. It is necessary to confirm before calculation whether the relationship between $\boldsymbol{I}$ and $\boldsymbol{S}$ is contradictory. When the state of the OSW of λ_q in Node p was $\mathrm{C_{LB}}$, the signal of λ_q transmitted from L3SW in Node p was looped back through the OSW and λ_q was not inputted into the AWGR. Thus, the matrix entry $i_{p,q}$ of $\boldsymbol{I}$ had to be 0. To confirm this, we define the detection matrix $\boldsymbol{D}$ as follows:

$$\begin{aligned} \boldsymbol{D} = \boldsymbol{I} \circ \boldsymbol{S} = (d_{p,q}) \quad & p = 1, \ldots, N\text{: node number} \\ & q = 1, \ldots, N\text{: wavelength number} \end{aligned} \tag{5}$$

where matrix entry $d_{p,q}$ was determined by multiplying $i_{p,q,}$ and $s_{p,q}$. When $d_{p,q}$ was not 0, it was observed that the signal of λ_q in Node p was not inputted into the AWGR as it was looped back to L3SW. Thus, entries of $\boldsymbol{I}$ or $\boldsymbol{S}$ were changed, with the result that $\boldsymbol{D}$ was 0. The calculation of path topology that includes transit nodes was performed for a matrix corresponding to each wavelength; next, $\boldsymbol{I}_q$, $\boldsymbol{S}_q$, and $\boldsymbol{L}_q$ were calculated.

First, the $\boldsymbol{I}_q$ corresponding to λ_q was calculated from $\boldsymbol{I}$. The $\boldsymbol{I}_q$ is expressed as follows:

$$\boldsymbol{I}_q = diag\left(i_{1,q}, i_{2,q}, \ldots, i_{N,q}\right) \tag{6}$$

The equation indicates $\boldsymbol{I}_q$, which is created by converting each diagonal element of an $N \times N$ identity matrix into each element $(i_{p,q})$ of the column corresponding to λ_q of $\boldsymbol{I}$. In the same manner, each $\boldsymbol{L}_q$ based on $\boldsymbol{L}$ was calculated. Thus, the $\boldsymbol{L}_q$ corresponding to λ_q and the element $l_{j,k}$ of $\boldsymbol{L}_q$ can be expressed as follows:

$$\begin{aligned} \boldsymbol{L}_q = (l_{j,k}) \quad & j = 1, \ldots, N\text{: source node number} \\ & k = 1, \ldots, N\text{: destination node number} \end{aligned} \tag{7}$$

$$l_{j,k} = \begin{cases} l_{j,k}, & q = r \\ 0, & q \neq r \end{cases} \tag{8}$$

The OSW state matrix $\boldsymbol{S}_q$ and its entries $t_{j,k}$ are expressed as follows:

$$\boldsymbol{S}_q = (t_{j,k}) \tag{9}$$

$$t_{j,k} = \begin{cases} e_{m,j}, & s_{p,q} = 0 \\ l_{j,m}, & s_{p,q} = 1 \end{cases}, \ m = 1, 2, \ldots, N \tag{10}$$

The equation shows that the mth column of $\boldsymbol{S}_q$ was equal to the mth column of the identity matrix when the state of the OSW of λ_q in Node m was $\mathrm{C_{PT}}$. Alternatively, the equation shows that the mth column of $\boldsymbol{S}_q$ was equal to the mth row of $\boldsymbol{L}_q$, when the state of the OSW was $\mathrm{C_{LB}}$. Here, $\boldsymbol{O}_q$ corresponding to λ_q is expressed as follows:

$$\begin{aligned} \boldsymbol{O}_q = (o_{j,k}) \quad & j = 1, \ldots, N\text{: source node number} \\ & k = 1, \ldots, N\text{: destination node number} \end{aligned} \tag{11}$$

and $\boldsymbol{O}_q$ is calculated using the following equation:

$$\boldsymbol{O}_q = \left(\boldsymbol{S}_q^z \cdot (\boldsymbol{L}_q)^T \cdot \boldsymbol{I}_q \right)^T \tag{12}$$

where z is the loopback number and $\boldsymbol{S}_q^z$ is an identity matrix if z is 0. T denotes the operation of matrix transposition. Finally, $\boldsymbol{O}$ is calculated as follows:

$$\boldsymbol{O} = \sum_{q=1}^{N} \boldsymbol{O}_q \tag{13}$$

where the element $o_{j,k}$ in $\boldsymbol{O}$ indicates the path topology of the AWG-STAR network and exhibits the source, transit, and destination nodes by multiplication of $i_{p,q}$ and $l_{j,k}$. The polynomial expression of $o_{j,k}$ that comprises the multiplication terms $i_{p,q}$ and $l_{j,k}$ shows path information between Nodes j and k. For example, the wavelength path from Nodes 1 to 3 was a direct path when $o_{j,k}$ was $i_{1,3}l_{1,3}$. Similarly, when $o_{j,k}$ was $i_{1,2}l_{1,2} + i_{1,3}l_{1,3}$, we obtain two wavelength paths, namely, one direct path from Nodes 1 to 3 and a loopback path from Nodes 1 to 3, transiting through Node 2. Therefore, the proposed calculation method can show network topology including transit nodes. Furthermore, the polynomial expression of $o_{j,k}$ showed path capacity or signal power by substituting capacity and power or loss thereof for $i_{p,q}$ and $l_{j,k}$. We observed that when path capacity and "1" were substituted for elements $i_{p,q}$ and $l_{j,k}$, respectively, $\boldsymbol{O}$ was obtained as path capacity. The proposed method expressed network topology so that it could also calculate network information based on topologies, such as distance and latency, and be helpful for a network controller that needed topology information. The proposed method minimizes the operating expenses for complex networks by clarifying path relations among nodes. However, since the proposed method outputs the wavelength path from the internal state of the OSW, it is impossible to calculate the required internal state of the OSW from the information between the nodes where the wavelength path is multiplexed. In addition, from the network management perspective, we need an interface easy for network administrators to manage, but previous proposals have only considered basic calculation methods. In this article, we propose a new method for calculating wavelength path routes and OSW states based on the previously proposed method and present an application with a graphical user interface (GUI) developed for network administrators. The rest of this article is organized as follows. In Section 3, we propose a new method for calculating wavelength path routes and OSW states based on the previously proposed method. In Section 4, we

show concrete examples using developed applications for network management. Finally, we summarize the findings of this study in Section 5.

3. **Description of the Calculation Method for the Required OSW State.** In this section, we propose a calculation method for the required OSW state to establish the multiplexed path by inputting the number of nodes and the nodes that need more paths. If we employ the inverse matrix calculation to know the required $\boldsymbol{S}$, we must know all matrices except $\boldsymbol{S}$ in advance, which is unrealistic. Thus, we propose a method to search for candidate OSW states to construct paths to be multiplexed and a method to select paths from the candidates. In this study, we consider multiplexing a single path, multiplexing multiple paths, and multiplexing in order of priority, as well as selecting the route that minimizes the number of transit nodes. First, we propose the calculation method to search for candidate OSW states. This is the common method to search in all cases. Afterward, we propose workflows for three cases. The method to calculate the candidate OSW states is as follows.

1) Input the number of nodes (N) in the AWG-STAR network and the nodes between which the wavelength paths are to be multiplexed (from Nodes x to y).
2) $\boldsymbol{I}$, $\boldsymbol{S}$, and $\boldsymbol{L}$, which are initial parameters, are obtained from the input information at the first step.
3) Set all elements except the xth row of $\boldsymbol{I}$ to 0 and all elements except the xth column of $\boldsymbol{S}$ to 1. Then, $\boldsymbol{I}$, $\boldsymbol{S}$, and $\boldsymbol{L}$ are as follows.

$$\boldsymbol{I} = \begin{pmatrix} 0 & 0 & \cdots & 0 \\ \vdots & \vdots & \ddots & \vdots \\ 0 & 0 & \cdots & 0 \\ i_{x,1} & i_{x,2} & \cdots & i_{x,N} \\ 0 & 0 & \cdots & 0 \\ \vdots & \vdots & \ddots & \vdots \\ 0 & 0 & \cdots & 0 \end{pmatrix} \tag{14}$$

$$\boldsymbol{S} = \begin{pmatrix} 1 & \cdots & 1 & 0 & 1 & \cdots & 1 \\ \vdots & \vdots & \vdots & \vdots & \vdots & \ddots & \vdots \\ 1 & \ldots & 1 & 0 & 1 & \cdots & 1 \end{pmatrix} \tag{15}$$

$$\boldsymbol{L} = \begin{pmatrix} \Lambda_1 & \Lambda_2 & \Lambda_3 & \cdots & \Lambda_r & \cdots & \Lambda_N \\ \Lambda_N & \Lambda_1 & \Lambda_2 & \cdots & \Lambda_{r-1} & \cdots & \Lambda_{N-1} \\ \Lambda_{N-1} & \Lambda_N & \Lambda_1 & \cdots & \Lambda_{r-2} & \cdots & \Lambda_{N-2} \\ \vdots & \vdots & \vdots & \ddots & \vdots & \ddots & \vdots \\ \Lambda_2 & \Lambda_3 & \Lambda_4 & \cdots & \Lambda_{r+1} & \cdots & \Lambda_1 \end{pmatrix} \quad r = 1, 2, \ldots, N \tag{16}$$

4) Next, we calculate $\boldsymbol{O}$ from Equations (12) and (13) based on [14] as follows:

$$\boldsymbol{O} = \begin{pmatrix} 0 & 0 & \cdots & 0 & \cdots & 0 \\ \vdots & \vdots & \ddots & \vdots & \ddots & \vdots \\ 0 & 0 & \cdots & 0 & \cdots & 0 \\ 0 & 0 & \cdots & X & \cdots & 0 \\ 0 & 0 & \cdots & 0 & \cdots & 0 \\ \vdots & \vdots & \ddots & \vdots & \ddots & \vdots \\ 0 & 0 & \cdots & 0 & \cdots & 0 \end{pmatrix} \tag{17}$$

$$X = \sum_{k=1}^{N} \lambda_k \prod_{l=1}^{LCM(|k-x|,N)/N} [\{x + (l-1)(k-1)\} \bmod N, \{x + l(k-1)\} \bmod N] \quad (18)$$

where the value of $\{x + (l-1)(k-1)\} \bmod N$ and $\{x + l(k-1)\} \bmod N$ are replaced N when the value is 0 in Equation (13). This shows the path of all incoming signals from Node x until they are looped back and output to Node x again. For example, when X is $\lambda_1(1,1) + \lambda_2(1,2)(2,3)(3,1) + \lambda_3(1,3)(3,2)(2,1)$, we obtain 3 wavelength paths, namely, paths from Node 1 to Node 1 via AWGR by λ_1, from Node 1 to Node 2 to Node 3 to Node 1 by λ_2, and from Node 1 to Node 3 to Node 2 to Node 1 by λ_3, which gives us the maximum loopback path for all wavelengths coming in from a single port.

5) From the result of this calculation, we can find the required OSW (Port, Lambda) by tracing the path to Node y.

Then, we propose a method to multiplex a single required path. This method is the most basic method for required OSW states because it is a common technique for searching for candidate OSW states, and it is very simple to select the shortest path among candidates. Figure 2 shows the workflow for searching the required OSW state and showing the result. In this case, the candidate OSW states are calculated using the proposed method, and the shortest path whose transit node is the least is selected. Figure 3 shows the workflow for searching multiplexing multiple paths. In this case, the candidate OSW states for each multiplexed path are calculated individually, and the optimum combination of candidates in which all paths can be established is selected. In this study, we employed a recursive algorithm to search for a feasible path. Figure 4 shows the workflow for searching multiplexing in order of priority. In this case, the candidate OSW state for each multiplexed path is calculated successively in order of priority and relocated paths and OSW states are locked not to change by low priority path.

The combination of the proposed OSW state calculation method and workflow enables path optimization under the condition that the numbers of multiplexed paths and priorities become more complex.

The three workflows shown in this paper use the basic path selection method of minimizing the number of transit nodes, but more advanced path selection is possible by applying path selection algorithms such as those in [15].

4. **Calculation Examples.** In this section, we use three concrete examples to illustrate the proposed matrix calculation method using developed applications. We developed two applications with GUI for network administrators based on our proposal in Section 2. The first application, which is used as the first example, employs the workflow in Figure 3, and the second application, which is used as the second and third examples, employs the workflow in Figure 4. These applications can suggest OSW states and show the result of path relocation. Table 1 shows the wavelength routing characteristics of an 8×8 AWGR. In the initial state, the nodes were assumed to be logically connected wavelength paths with a full-mesh topology.

For the first example, we made some changes to the wavelength path topology and network capacity of the network to increase capacities from Nodes 1 to 2, from Nodes 7 to 8, and from Nodes 4 to 5. In this case, we assumed each path has the same priority, so we used brute force calculation. Figure 5 shows the GUI for input conditions. The number of nodes in the AWG-STAR network, number of multiplexed paths, and multiplexed nodes are input. The GUI also shows OSWs that need to change state after calculation. Figure 6 shows the result of network topology after changing the OSWs. This GUI shows the result of a calculation based on [14] when OSW states are changed as Figure 5. The

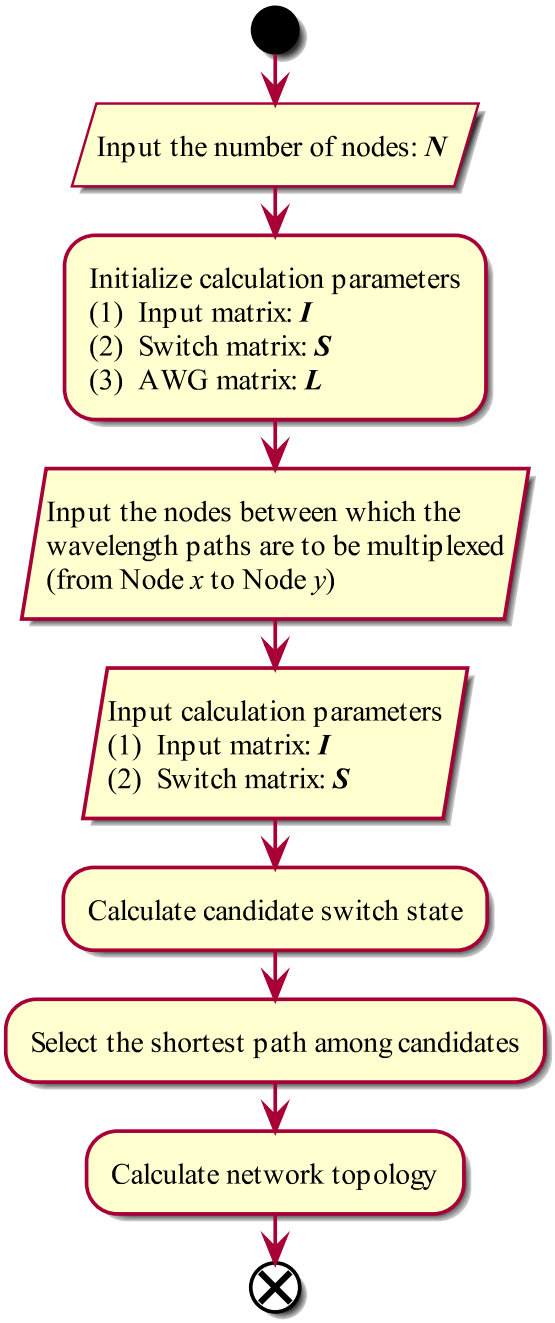

FIGURE 2. Workflow for searching the required OSW state and showing the result

representation of each element is the same as X. In this example, twelve OSW states are changed as Figure 5, and Figure 6 shows that three wavelength paths are multiplexed as inputted in Figure 5. On the other hand, there are no paths if elements are 0 shown as in Figure 6.

In the second example, we made some changes to the wavelength path topology and network capacity of the network to increase capacities from Nodes 1 to 2, from Nodes 7 to 8, and from Nodes 5 to 4. In this case, the multiplexed paths were prioritized, so we input them in order of priority in the GUI. Figure 7 shows the GUI for input conditions. The number of nodes in the AWG-STAR network, number of multiplexed paths, and multiplexed nodes are input. The GUI also shows OSWs that need change state after

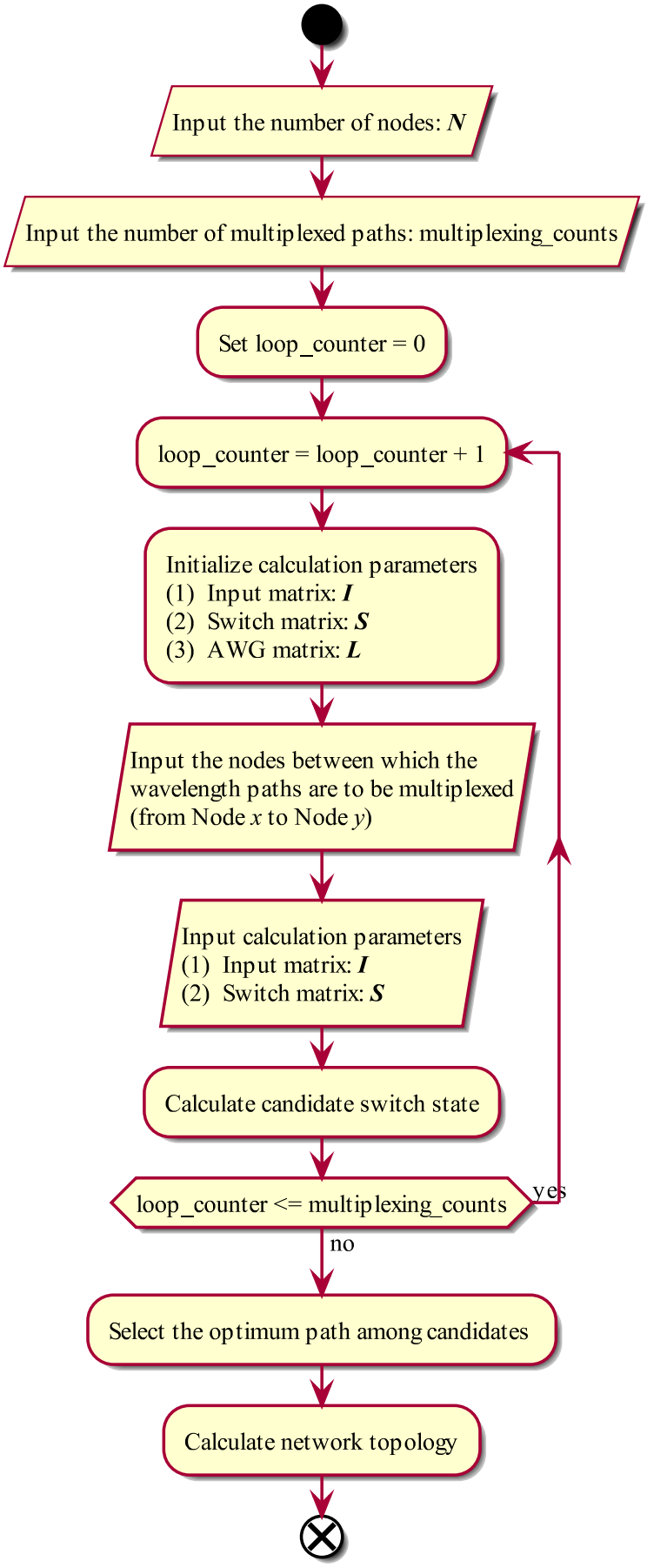

FIGURE 3. Workflow for searching multiplexing multiple paths

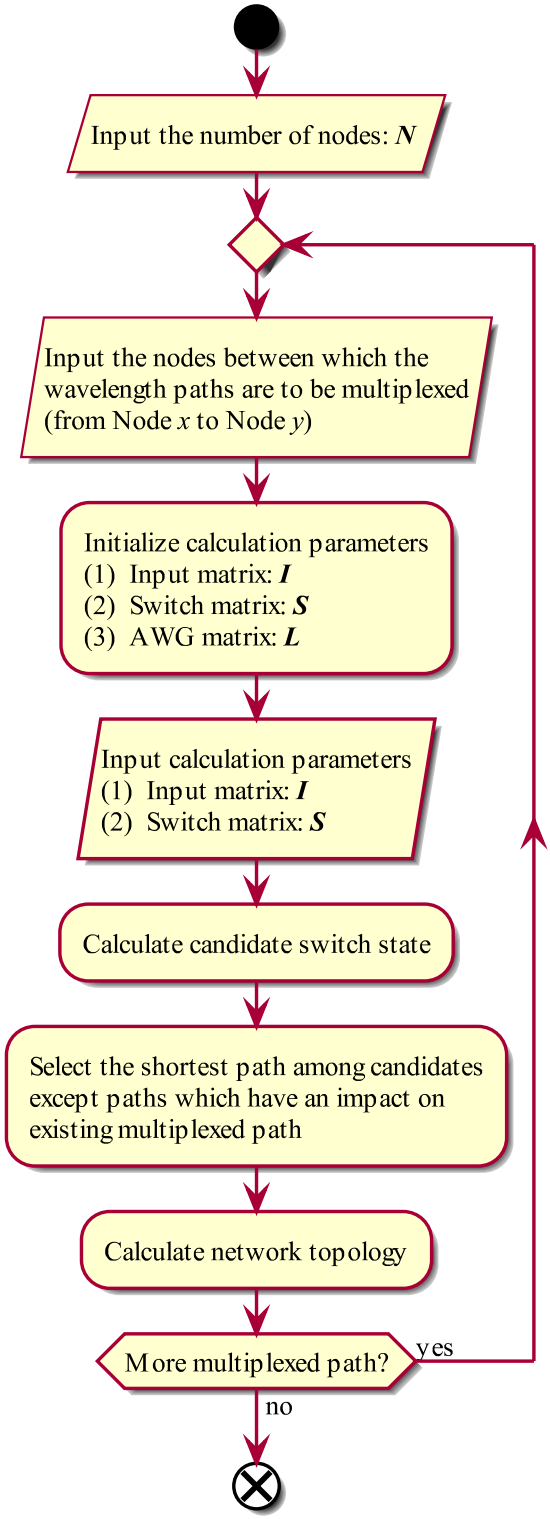

FIGURE 4. Workflow for searching multiplexing in order of priority

calculating. For a feasible candidate of OSW state, the GUI shows the result as "cannot change switch". In this case, all candidates were used at a higher priority multiplexed path. Figure 8 shows the result of network topology after changing the OSWs. This GUI shows the result of a calculation based on [14] when OSW states are changed as Figure 7. In this example, six OSW states are changed as Figure 5 and Figure 8 shows that two

TABLE 1. Wavelength routing table in an 8×8 AWGR

AWGR port	Out-1	Out-2	Out-3	Out-4	Out-5	Out-6	Out-7	Out-8
In-1	λ_1	λ_2	λ_3	λ_4	λ_5	λ_6	λ_7	λ_8
In-2	λ_8	λ_1	λ_2	λ_3	λ_4	λ_5	λ_6	λ_7
In-3	λ_7	λ_8	λ_1	λ_2	λ_3	λ_4	λ_5	λ_6
In-4	λ_6	λ_7	λ_8	λ_1	λ_2	λ_3	λ_4	λ_5
In-5	λ_5	λ_6	λ_7	λ_8	λ_1	λ_2	λ_3	λ_4
In-6	λ_4	λ_5	λ_6	λ_7	λ_8	λ_1	λ_2	λ_3
In-7	λ_3	λ_4	λ_5	λ_6	λ_7	λ_8	λ_1	λ_2
In-8	λ_2	λ_3	λ_4	λ_5	λ_6	λ_7	λ_8	λ_1

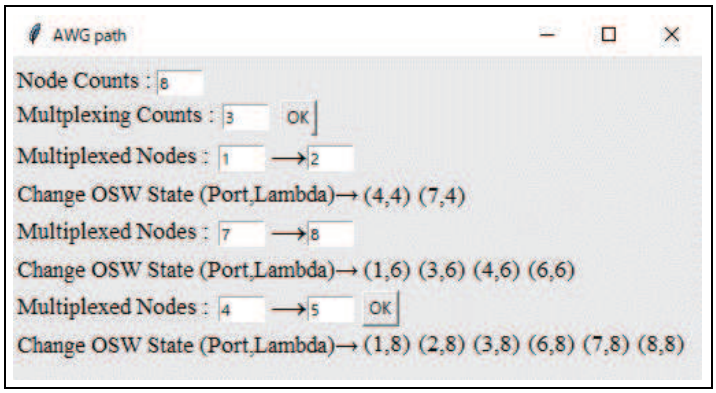

FIGURE 5. GUI for inputting conditions in the first sample

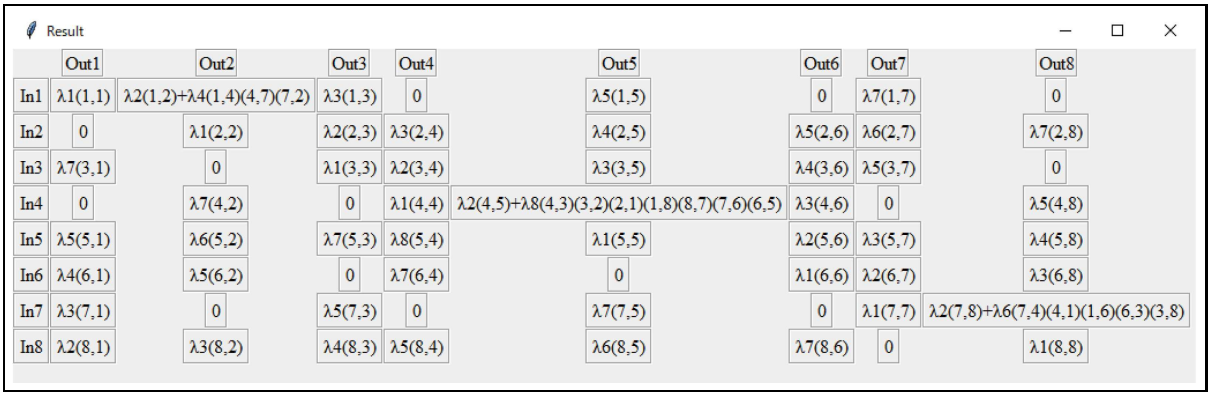

FIGURE 6. GUI for network topology after path reconfiguration in the first sample

wavelength paths are multiplexed as inputted in Figure 5. However, the wavelength path from Nodes 5 to 4 cannot be established because candidates of OSW states do not exist. On the other hand, there are no paths if elements are 0 shown as in Figure 8.

In the third example, we made some changes to the wavelength path topology and network capacity of the network to increase capacities from Nodes 1 to 2 as much as possible. Figure 9 shows the GUI for input conditions. The number of nodes in the AWG-STAR network, number of multiplexed paths, and multiplexed nodes are input. The GUI also shows OSWs that need a change state after calculating. When we input four times, GUI shows "cannot change switch" because the candidates have only three. Figure 10 shows the result of network topology after changing the OSWs. This GUI shows the result of a calculation based on [14] when OSW states are changed as Figure 9. In this example, twelve OSW states are changed as Figure 9 and Figure 10 shows

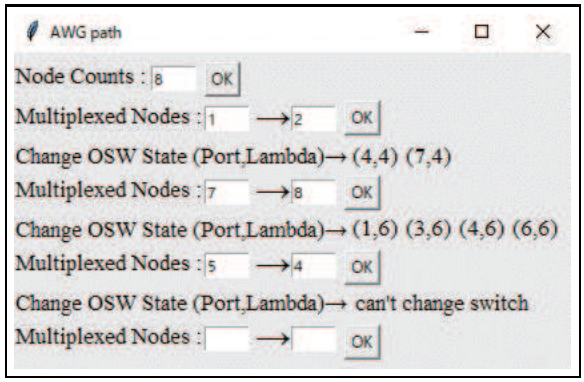

FIGURE 7. GUI for inputting conditions in the second sample

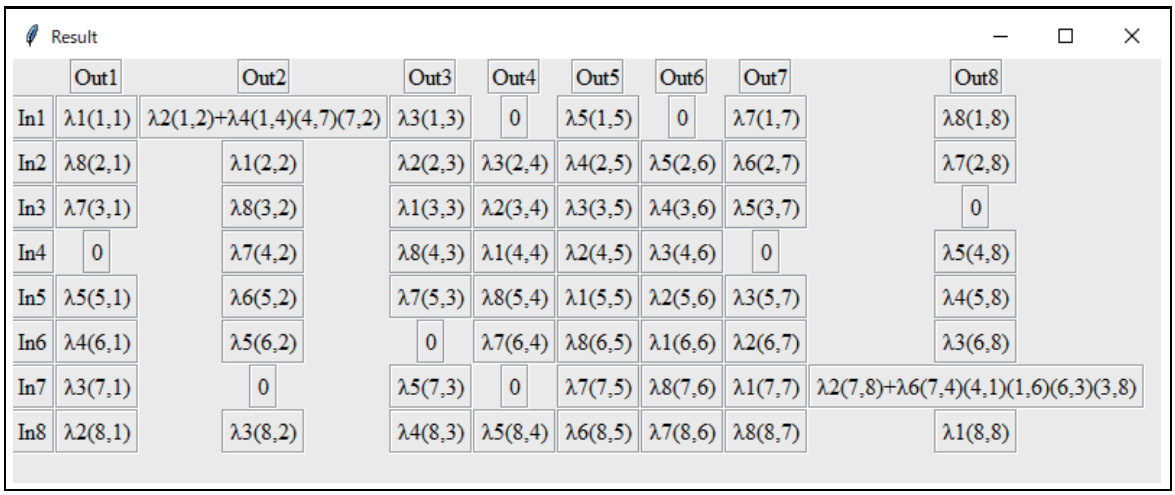

FIGURE 8. GUI for network topology after path reconfiguration in the second sample

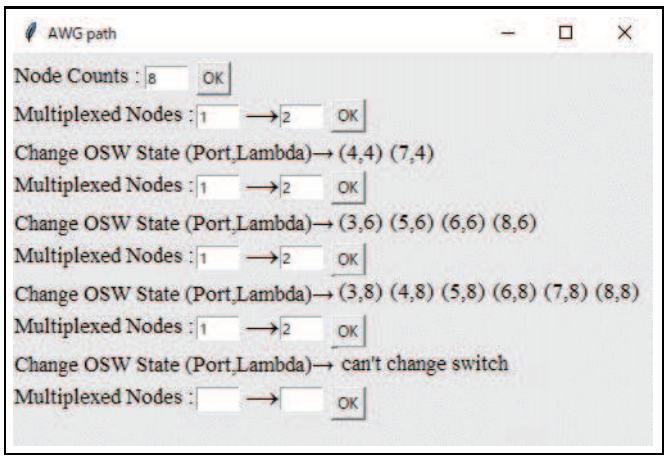

FIGURE 9. GUI for inputting conditions in the third sample

that one wavelength path is multiplexed threefold as inputted in Figure 9. However, the wavelength path from Nodes 1 to 2 cannot be multiplexed fourfold because candidates of OSW states do not exist. On the other hand, there are no paths if elements are 0 shown as in Figure 10.

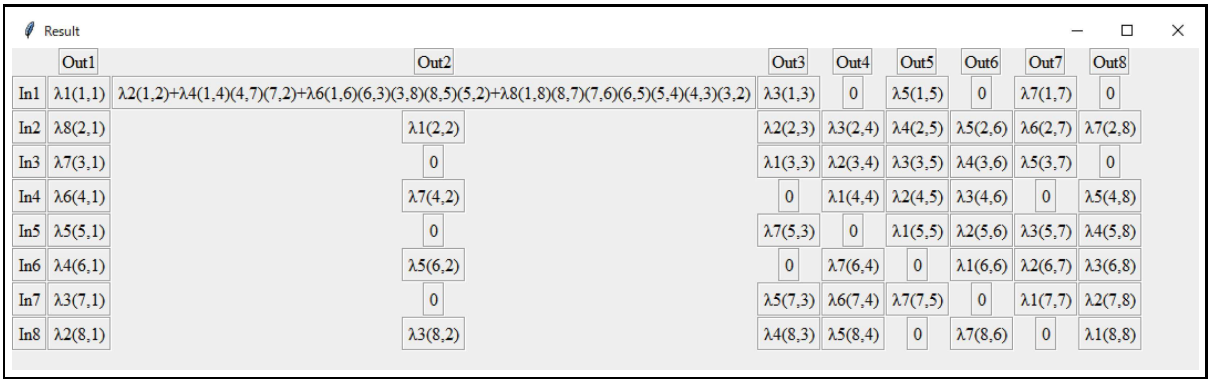

FIGURE 10. GUI for network topology after path reconfiguration in the third sample

5. **Conclusions.** We proposed a new method for calculating wavelength path routes and OSW states based on our previously proposed method [14] and presented an application with GUI developed for network administrators. Further, we used concrete examples to illustrate the applications of the newly proposed method using an 8×8 AWG-STAR network. The newly proposed method calculated OSW state to reconfigure the required topology, and the developed applications automatically expressed network topology. Since the conventional method [14] outputs the wavelength path from the internal state of the OSW, it is impossible to calculate the required internal state of the OSW from the information between the nodes where the wavelength path is multiplexed. The newly proposed method makes it possible to not only calculate the current topology from the current state of the devices but also to calculate the required switch state from the required topology, making it possible to not only understand the current state but also to plan the design of the network. The newly proposed method minimizes the operating expenses for complex networks by calculating required OSW states because network configuration is based on required network topology. Consequently, we aimed to achieve automatic relocation and reduce operating expenses of the AWG-STAR network with a loopback function.

Acknowledgment. This work was supported by JSPS KAKENHI Grant Number 16K06 306.

REFERENCES

[1] Cisco, *Global Cloud Index Projects Cloud Traffic to Represent 95 Percent of Total Data Center Traffic by 2021*, https://newsroom.cisco.com/press-release-content?type=webcontent&articleId=1908858, Accessed in August, 2021.

[2] B. Mukherjee, WDM optical communication networks: Progress and challenges, *IEEE Journal on Selected Areas in Communications*, vol.18, no.10, pp.1810-1824, 2000.

[3] J. Sakaguchi, Y. Awaji, N. Wada, A. Kanno, T. Kawanishi, T. Hayashi, T. Taru, T. Kobayashi and M. Watanabe, Space division multiplexed transmission of 109-Tb/s data signals using homogeneous seven-core fiber, *Journal of Lightwave Technology*, vol.30, no.4, pp.658-665, 2012.

[4] K. Noguchi, A. Okada, S. Kamei, S. Suzuki and M. Matsuoka, Temperature control-free full-mesh wavelength routing network (AWG-STAR) with CWDM AWG-router, *Journal of Lightwave Technology*, vol.23, no.4, pp.1568-1575, 2005.

[5] K. Noguchi, Scalability of full-mesh WDM AWG-STAR network, *IEICE Trans. Commun.*, vol.E86-B, no.5, pp.1493-1497, 2003.

[6] K. Jones, Enabling technologies for in-router DWDM interfaces for intra-data center networks, *Proc. of Optical Fiber Communication Conference 2019*, San Diego, CA, USA, 2019.

[7] M. Xu, J. Diakonikolas, E. Modiano and S. Subramaniam, A hierarchical WDM-based scalable data center network architecture, *Proc. of 2019 IEEE International Conference on Communications*, Shanghai, China, pp.327-338, 2019.
[8] G. Wang, D. G. Andersen, M. Kaminsky, K. Papagiannaki, T. E. Ng, M. Kozuch and M. Ryan, C-through: Part-time optics in data centers, *Proc. of the ACM SIGCOMM 2010 Conference*, New Delhi, India, pp.327-338, 2010.
[9] N. Farrington, G. Porter, S. Radhakrishnan, H. H. Bazzaz, V. Subramanya, Y. Fainman, G. Papen and A. Vahdat, Helios: A hybrid electrical/optical switch architecture for modular data centers, *Proc. of the ACM SIGCOMM Conference*, New Delhi, India, pp.339-350, 2010.
[10] H. Liu, F. Lu, A. Forencich, R. Kapoor, M. Tewari, G. M. Voelker, G. Papen, A. C. Snoeren and G. Porter, Circuit switching under the radar with REACToR, *Proc. of the 11th USENIX Symposium on Networked Systems Design and Implementation*, Seattle, WA, USA, pp.1-15, 2014.
[11] M. Ghobadi, R. Mahajan, A. Phanishayee, N. Devanur, J. Kulkarni, G. Ranade, P.-A. Blanche, H. Rastegarfar, M. Glick and D. Kilper, Projector: Agile reconfigurable data center interconnect, *Proc. of the ACM SIGCOMM Conference*, Florianopolis, Brazil, pp.216-229, 2016.
[12] M. Yamaguchi, O. Koyama, H. Maruyama, T. Niihara and M. Yamada, Matrix representation for wavelength path relocation in AWG-STAR network with loopback function, *International Journal of Innovative Computing, Information and Control*, vol.12, no.3, pp.833-845, 2016.
[13] T. Niihara, O. Koyama, Y. Tomioka, S. Aso, Y. Ogura and M. Yamada, Calculation method for wavelength path with transit nodes and its accumulated optical loss in AWG-STAR network with loopback function, *International Journal of Innovative Computing, Information and Control*, vol.14, no.4, pp.1253-1265, 2018.
[14] M. Yamaguchi, O. Koyama, K. Ikeda and M. Yamada, Calculation method for wavelength path planning in arrayed waveguide grating – STAR network, *International Journal of Innovative Computing, Information and Control*, vol.16, no.6, pp.1959-1971, 2020.
[15] Y.-J. Lee, A path selection model considering path latency in the communication network with geographically correlated failures, *ICIC Express Letters*, vol.13, no.9, pp.789-796, 2019.

Author Biography

Kento Oyama received M.E. degrees from Osaka Prefecture University (OPU), Japan, in 2021. His research interests include a software for calculating wavelength path topologies and optical switch conditions in IP over AWG-STAR network.

Minoru Yamaguchi received B.E. and M.E. degrees from Osaka Prefecture University (OPU), Japan, in 2014 and 2016, respectively. He is currently enrolled in Ph.D. program in Engineering at OPU. His research interests include computation and control methods for wavelength path management in IP over AWG-STAR network.

Osanori Koyama received B.E., M.E. and Ph.D. degrees from Osaka Prefecture University (OPU), Japan, in 1999, 2001 and 2013 respectively. Currently he works at Photonic Innovative Systems Research Group as associate professor in OPU. His research interests include design and control issues related to optical IP networks based on software defined networking, and optical fiber sensing system over IP network.

Keigo Mino received B.E. and M.E. degrees from Osaka Prefecture University (OPU), Japan, in 2019 and 2021, respectively. His research interests include a router/switch control system using single-board computer supported OpenFlow functions.

Akihiro Imae received B.E. degree from Osaka Prefecture University (OPU), Japan, in 2020. Currently he is a master's student of engineering at OPU. His main research interests include Web-based network control and management based on software defined networking using single-board computer.

Ippei Tomo received the B.E. degree from Osaka Prefecture University (OPU), Japan, in 2021. Currently he is a research member of Photonic Innovative Systems Research Group in OPU. His interests include software develop for wavelength path management in IP over AWG-STAR network.

Kanami Ikeda is assistant professor of the Department of Electrical & Information Systems, Osaka Prefecture University, Japan. She received Ph.D. degree in engineering from the University of Electro-Communications, Japan in 2018. Her research interests include optical communications and networking, optical information processing, and optical sensing. She is a member of Optica.

Makoto Yamada is professor of the Department of Electrical & Information Systems, Osaka Prefecture University (OPU), Japan. He received B.E. and M.E. degrees in electrical engineering from the Technical University of Nagaoka, Niigata, Japan in 1983 and 1985, respectively. He joined NTT Laboratories in 1985, where he was engaged in research on planar lightwave circuits. Since 1989, he has been engaged in research on optical fiber amplifiers. In 1999, he received D.E. degree in the area of optical amplifiers. He joined OPU in 2008, and has been the professor since 2013. His research interests include design & control for optical amplifiers and other components in optical networks.

Prof. Yamada is a Senior Member of the Institute of Electrical and Electronics Engineers (IEEE), a Senior Member of the Institute of Electronics, Information and Communication Engineers of Japan (IEICE), a Member of Japan Society of Applied Physics, and a Fellow of the Optical Society (OSA).

Prof. Yamada received the Paper Award (1994) from the IEICE, the Electronics Letters Premium (1997) from the Institution of Electrical Engineers, and the Sakurai Prize (1998) and Meritorious Award of 40th foundation anniversary (2021) from the Optoelectronics Industry and Technology Development Association (OITDA).